

## The scandium–ruthenium phase diagram

V.N. Eremenko, V.G. Khorujaya \*, P.S. Martsenyuk, K. Ye. Korniyenko

*I.N. Frantsevich Institute for Problems of Materials Science, Academy of Sciences of Ukraine, Krzyzanovsky St. 3, 252180 Kiev, Ukraine*

Received 4 May 1994; in final form 28 June 1994

### Abstract

The constitutional diagram of the Sc–Ru system is investigated using metallography, X-ray diffraction, microprobe and differential thermal analysis data as well as alloy melting-point data measured according to the Pirani–Alterthum method. The existence of four intermediate phases in the system, namely ScRu<sub>2</sub> (MgZn<sub>2</sub>-type structure), ScRu (CsCl), Sc<sub>11</sub>Ru<sub>4</sub> (Zr<sub>11</sub>Os<sub>4</sub>) and Sc<sub>57</sub>Ru<sub>13</sub> (Sc<sub>57</sub>Rh<sub>13</sub>), is substantiated. Sc<sub>3</sub>Ru<sub>3</sub> and Sc<sub>2</sub>Ru were observed for the first time. Their crystal structures were attributed by us to the Mn<sub>5</sub>Si<sub>3</sub> and Ti<sub>2</sub>Ni types respectively. The existence of the phase Sc<sub>3</sub>Ru, mentioned in the literature, was not verified. The ScRu<sub>2</sub>, ScRu and Sc<sub>57</sub>Ru<sub>13</sub> phases melt congruently with the solidus curve maxima at 1820 °C, 1760 °C and 1290 °C respectively. The Sc<sub>5</sub>Ru<sub>3</sub>, Sc<sub>2</sub>Ru and Sc<sub>11</sub>Ru<sub>4</sub> phases form by the peritectic reactions at 1300 °C, 1160 °C and 1130 °C respectively. The formation of the Sc<sub>44</sub>Ru<sub>7</sub> phase is assumed to occur via a solid state reaction at 950 °C. Coordinates of four eutectic points and one eutectoid point are determined.

*Keywords:* Scandium; Ruthenium; Phase diagrams

### 1. Introduction

The existence of the Laves phase ScRu<sub>2</sub> (MgZn<sub>2</sub>-type structure;  $a = 5.119$  Å and  $c = 8.542$  Å [1];  $a = 5.135$  Å and  $c = 8.525$  Å [2]) has been reported from X-ray diffraction studies. A phase based on the equiatomic compound ScRu with the CsCl-type structure and lattice period  $a = 3.200$  Å, was reported in [3]. On the basis of calculations, the existence of Sc<sub>3</sub>Ru has been suggested [4]. The complete Sc–Ru phase diagram, given in [5], contained three considered compounds. In later investigations [6–8] the existence of Sc<sub>11</sub>Ru<sub>4</sub> and Sc<sub>57</sub>Ru<sub>13</sub> was detected by X-ray diffraction studies of single crystals having these stoichiometries. Also the unsuccessful search for Sc<sub>44</sub>Ru<sub>7</sub> was reported. In the present investigation we have tried to remove the discrepancies existing in the literature concerning the Sc–Ru system.

### 2. Experimental methods

The investigated alloys were prepared by arc melting with a non-consumable tungsten electrode on a water-cooled copper hearth in an atmosphere of purified argon. The starting materials were ruthenium powder

with a nominal purity of 99.95%, preliminarily sintered in vacuum at 1500 °C and then subjected to arc remelting, scandium metal (the impurity content did not exceed 0.15%, excluding an oxygen impurity of 1.3 wt.%). During the melting process, evaporation of the more volatile component, i.e. scandium, took place. As a result of this the total weight losses during melting, in some cases 2 wt.%, were attributed to losses of scandium. After preliminary determinations of the solidus temperatures for the as-cast samples, they were homogenized by heating them in an atmosphere of purified argon for 50 h at 1500 °C or for 100–200 h at 900 °C, depending on the composition.

The alloys were investigated by metallography, X-ray diffraction, microprobe analysis and differential thermal analysis (DTA). The temperatures of the beginning of melting were determined also by the method of Pirani and Alterthum [9].

The microstructural examination of the alloys with 45–100 at.% Ru was carried out after electrochemical etching in a solution containing hydrochloric acid and glycerine in a volume ratio of 2:1. For the scandium-rich alloys, chemical etching in a glycerine solution of nitric acid (HNO<sub>3</sub>:glycerine = 1:3) was used. Microprobe analyses were conducted using a JEOL Superprobe-733 instrument, which gave an accuracy of  $\pm 1$  at.%. X-ray diffraction studies of the alloys were conducted by the Debye–Scherrer method using a Debye focusing

\* Corresponding author.

camera with a diameter of 57.3 mm and Cu K $\alpha$  radiation as well as using a diffractometer for planar sections. The calculation of the lattice parameters was carried out by means of a computer program based on the method of Cohen [10] and Hess [11]. For thermographic studies a W-(W-20%Re) wire thermocouple served as a pick-up.

### 3. Results and discussion

The results of the current investigation have been presented in the form of a constitutional diagram of the Sc–Ru system shown in Fig. 1. It is believed to be accurate to within  $\pm 1$  at.% and  $\pm 20$  °C. Crystallographic data for the intermediate phases existing in the system have been listed in Table 1. We substantiated the formation of the Laves phase ScRu<sub>2</sub> ( $\lambda_1$ ) in the system. However, in contrast with [5], we determined that ScRu<sub>2</sub> melts congruently at 1820 °C. This phase forms a eutectic with the solid solution based on ru-

thenium:  $L \rightleftharpoons \text{ScRu}_2 + \langle \text{Ru} \rangle$ . The eutectic coordinates, in contrast with those reported in the literature (83 at.% Ru and 1790 °C) were determined by us as 76 at.% Ru and 1760 °C. The temperature of 1760 °C was found by two independent methods, namely DTA and the Pirani–Alterthum method (Table 2). The composition at the eutectic point was obtained on the basis of microprobe analysis results for ‘as-cast’ alloys containing 72.8 and 81.4 at.% Ru and located in different directions from the eutectic point (Table 3). The eutectic composition was verified also from the entirely eutectic microstructure of the alloy with 76.6 at.% Ru (Fig. 2(a)). The solubility of scandium in ruthenium was determined also by the microprobe analysis method. Its value is 2 at.% Sc at 1750 °C (Table 3). The congruent nature of the crystallization of the phase based on ScRu<sub>2</sub> follows from the shape of its liquidus curve within the composition field 54–77 at.% Ru (Fig. 3, curves a–c), derived from the DTA data (Table 2), and from the eutectic crystallization structures of the cast alloys within this compositional range (Fig. 2(b)). It should be noted that the eutectic mixture looks like a degenerate eutectic, because the compositions of the liquid and one of the solid phases of the equilibrium  $L \rightleftharpoons \text{ScRu} + \text{Sc}_2\text{Ru}$  are similar. The temperature at which this reaction took place was determined by DTA and

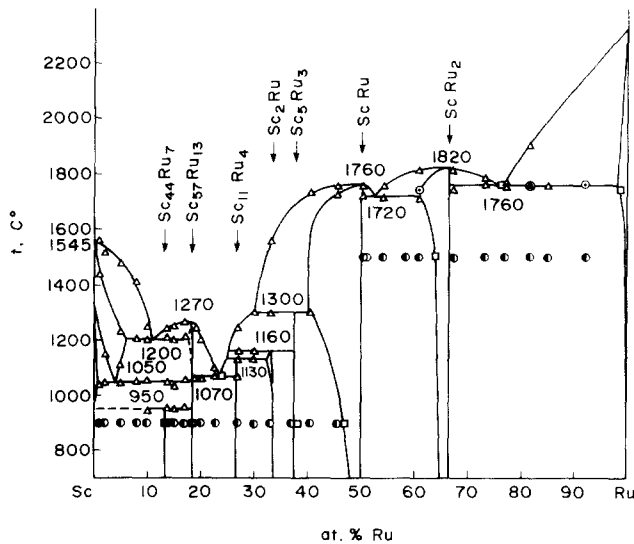


Fig. 1. The Sc–Ru phase diagram: O, single phase; ●, two phases; ○, solidus; □, microprobe; Δ, thermal analysis.

Table 1  
Crystallographic data for Sc–Ru intermediate phases

Intermediate phase	Space group	Structure type	Lattice parameters (Å)	
			<i>a</i>	<i>c</i>
ScRu <sub>2</sub>	<i>P6<sub>3</sub>/mmc</i>	MgZn <sub>2</sub>	5.13	8.52
ScRu	<i>Pm3m</i>	CsCl	3.20	–
Sc <sub>5</sub> Ru <sub>3</sub>	<i>P6<sub>3</sub>/mcm</i>	Mn <sub>5</sub> Si <sub>3</sub>	8.03	5.48
Sc <sub>2</sub> Ru	<i>Fd3m</i>	Ti <sub>2</sub> Ni	12.30	–
Sc <sub>11</sub> Ru <sub>4</sub>	<i>Fm3m</i>	Zr <sub>11</sub> Os <sub>4</sub>	13.42	–
Sc <sub>57</sub> Ru <sub>13</sub>	<i>Pm3</i>	Sc <sub>57</sub> Rh <sub>13</sub>	14.38	–
Sc <sub>44</sub> Ru <sub>7</sub>	<i>F43m</i>	Mg <sub>44</sub> Rh <sub>7</sub>	20.75	–

Table 2  
Temperature of phase transitions in alloys of the Sc–Ru system

Ru (at.%)	Phase transition temperature (°C)			
	By DTA		By Pirani–Alterthum method, solidus	
	Solidus state	Solidus		Liquidus
1	1040	1435	1560	
2	1045, 1150	–	–	
5	1045, 1110	1230	1480	
8	1060	1205	1410	
10	945, 1065	1205	1255	
13.8	955, 1045	1212	1240	
15	950, 1035	1200	1250	
17	965, 1070	1210	1265	
18.7		1055	1247	
20		1055	1200	
23		1070	1100	
26.8		1065	1245	
30		1130	1300	
33		1160	1560	
40.6		1300	1740	
45.5		1730	1755	
50.1		1720	1750	
54		1720	1760	
60.7		1710	1815	1740
67.3		1740	1815	
72.8		1760	1780	
76.6		1760	1770	
81.4		1760	1905	1760
84.7		1765		
91.7				1770

Table 3  
Microprobe analyses

Ru (at.%)	Heat treatment temperature (°C)	Phases	Ru content (at.%)
13.8	900	Sc <sub>44</sub> Ru <sub>7</sub> Sc <sub>57</sub> Ru <sub>13</sub>	13.9 18.3
23.0	As cast	Eutectic (Sc <sub>11</sub> Ru <sub>4</sub> + Sc <sub>57</sub> Ru <sub>13</sub> )	24.0
26.8	As cast	Sc <sub>3</sub> Ru <sub>3</sub> Sc <sub>2</sub> Ru Sc <sub>11</sub> Ru <sub>4</sub>	38.0 32.8 26.0
33.0	As cast	ScRu Sc <sub>3</sub> Ru <sub>3</sub> Sc <sub>2</sub> Ru	45.9 38.0 32.8
40.6	900	ScRu Sc <sub>5</sub> Ru <sub>3</sub>	47.4 37.7
51.0	As cast	ScRu Eutectic (ScRu + ScRu <sub>2</sub> )	50.0 52.0
54.0	As cast	ScRu <sub>2</sub> Eutectic (ScRu <sub>2</sub> + ScRu)	62.0 52.2
58.3	1500	ScRu <sub>2</sub> ScRu	64.6 50.0
72.8	As cast	ScRu <sub>2</sub> Eutectic (ScRu <sub>2</sub> + <Ru>)	67.3 76.3
76.6	As cast	Eutectic (ScRu <sub>2</sub> + <Ru>)	75.6
81.4	As cast	<Ru> Eutectic (<Ru> + ScRu <sub>2</sub> )	98.7 75.8
	1750	<Ru> ScRu <sub>2</sub>	98.2 67.4

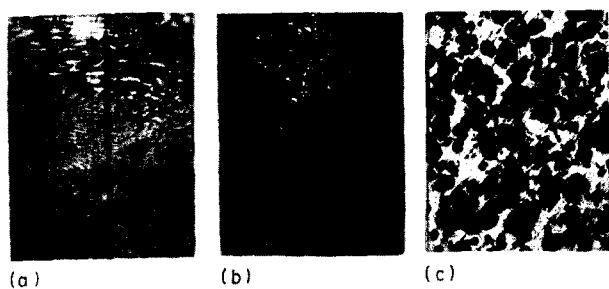


Fig. 2. Microstructure of alloys of the Sc–Ru system: (a) 76 at.% Ru, cast, eutectic (ScRu<sub>2</sub> + <Ru>); (b) 51 at.% Ru, cast, ScRu + eutectic (ScRu + ScRu<sub>2</sub>); (c) 8 at.% Ru, cast,  $\beta$ -Sc + eutectic ( $\beta$ -Sc + Sc<sub>57</sub>Ru<sub>13</sub>). (Magnifications: (a) 1000; (b), (c) 200.)

found to be equal to 1720 °C. The eutectic composition was established by microprobe analysis of hypoeutectic and hypereutectic alloys, containing 51 and 54 at.% Ru, and also by the point of intersection of the ScRu and ScRu<sub>2</sub> liquidus curves plotted from the DTA data

(Table 2). The phase based on the equiatomic compound ScRu melts congruently, which is in agreement with [5]. However, in contrast with 2100 °C, observed in [5], the liquidus and solidus maxima are determined by us as 1760 °C. The correctness of this value is confirmed by the fact that the samples containing 45 and 51 at.% Ru, after heating to 1830 °C, were melted completely (Fig. 3, curve d). Both ScRu and ScRu<sub>2</sub> have extensive homogeneity regions at subsolidus temperatures (about 8 at.% for ScRu and about 5 at.% for ScRu<sub>2</sub>). The upper limits of the ruthenium content of these phases in the corresponding homogeneity regions are almost equivalent to their stoichiometric compositions, whereas the lower limits extend into the scandium-rich compositional field. On decrease in the temperature the homogeneity regions of the phases ScRu and ScRu<sub>2</sub> become narrower. So, at 1500 °C according to the microprobe analysis data for the alloy containing 58.3 at.% Ru, the lower limit of the ruthenium content of ScRu<sub>2</sub> is 65 at.% (Table 3). The microprobe analysis of the alloy with 40.6 at.% Ru, annealed at 900 °C, gives evidence of the fact that the ScRu homogeneity range on the scandium side extends up to 47 at.% Ru at this temperature (Table 3). The lattice spacings within the limits of the homogeneity regions are believed

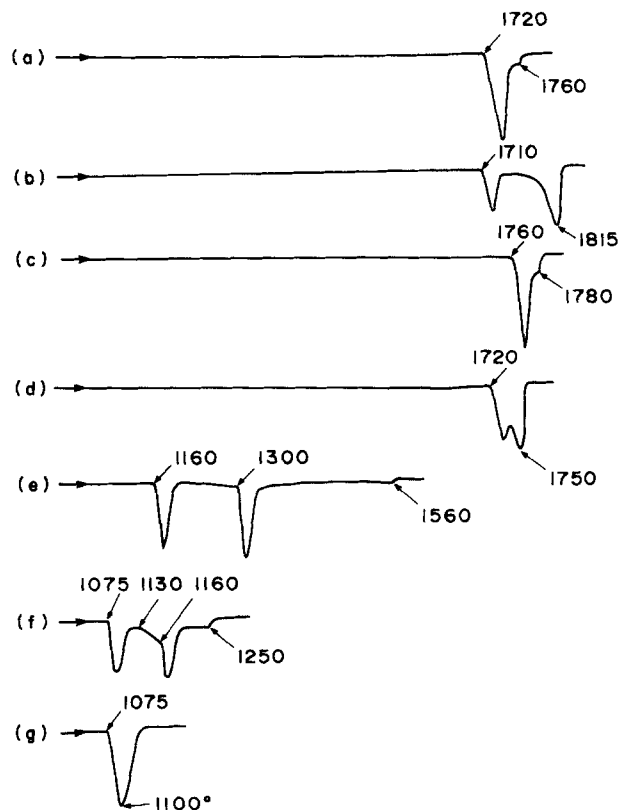


Fig. 3. Heating curves of some alloys of the Sc–Ru system: curve a, 54 at.% Ru, 1500 °C; curve b, 60.7 at.% Ru, 1500 °C; curve c, 72.8 at.% Ru, cast; curve d, 50.1 at.% Ru, 1500 °C; curve e, 33 at.% Ru, cast; curve f, 26.8 at.% Ru, 900 °C; curve g, 23 at.% Ru, cast.

to be accurate to within  $\pm 0.02 \text{ \AA}$  (within the limits of the accuracy of the measurements).

The phase equilibria in the Sc–Ru system for more than 50 at.% Sc have a complicated character and are completely different from those reported in [5]. We determined the intermediate phases  $\text{Sc}_5\text{Ru}_3$  and  $\text{Sc}_2\text{Ru}$  for the first time and confirmed the existence of  $\text{Sc}_{11}\text{Ru}_4$  and  $\text{Sc}_{57}\text{Ru}_{13}$ . A phase of the stoichiometry  $\text{Sc}_3\text{Ru}$  was not found.

So, the microprobe analysis of the cast alloys with 33 and 26.8 at.% Ru showed that in the first alloy a small amount of the primary dendrites corresponds to the ScRu phase. Successively two other phases had formed, conforming to the stoichiometries  $\text{Sc}_5\text{Ru}_3$  and  $\text{Sc}_2\text{Ru}$  (Table 3). The second alloy (26.8 at.% Ru) contains already the primary dendrites of the 5:3 phase while  $\text{Sc}_2\text{Ru}$  and  $\text{Sc}_{11}\text{Ru}_4$  had formed in it by peritectic reactions (Table 3). DTA of this alloy indicates that the reaction  $\text{L} + \text{ScRu} \rightleftharpoons \text{Sc}_5\text{Ru}_3$  proceeds at 1300 °C and the reactions  $\text{L} + \text{Sc}_5\text{Ru}_3 \rightleftharpoons \text{Sc}_2\text{Ru}$  and  $\text{L} + \text{Sc}_2\text{Ru} \rightleftharpoons \text{Sc}_{11}\text{Ru}_4$  at 1160 °C and 1130 °C respectively (Fig. 3, curves e and f). These results agree with the X-ray diffraction data. So, in the metallographically two-phase alloy with 40.6 at.% Ru, annealed at 900 °C for 100 h, besides the CsCl-type lattice reflections (ScRu phase) a complete reflection set, belonging to the  $\text{Mn}_5\text{Si}_3$ -type lattice structure is present (Table 4). Annealed at similar conditions, the two-phase alloys containing 33 and 26.8 at.% Ru contain reflections belonging to  $\text{Sc}_2\text{Ru}$  and  $\text{Sc}_{11}\text{Ru}_4$  ( $\text{Zr}_{11}\text{Os}_4$ -type structure). The crystalline structure of the phase  $\text{Sc}_2\text{Ru}$  was attributed by us to the  $\text{Ti}_2\text{Ni}$  type (Table 5).

The microprobe investigation of the cast alloy with 23 at.% Ru revealed the presence of small amounts of primary dendrites, the composition of which, by microprobe analysis, was determined as belonging to  $\text{Sc}_{57}\text{Ru}_{13}$ . Besides this, a eutectic with 24 at.% Ru (Table 3), corresponding to the transformation  $\text{L} \rightleftharpoons \text{Sc}_{11}\text{Ru}_4 + \text{Sc}_{57}\text{Ru}_{13}$  was found. According to the DTA data (using only the heating curve for this alloy (Fig. 3, curve g)), this eutectic reaction takes place at

Table 4  
 $\text{Sc}_5\text{Ru}_3$  X-ray diffraction data

$\sin^2\theta$	Relative intensity	<i>h k l</i> planes
0.0381	w	1 1 0
0.0463	w	2 0 0
0.0574	m	1 1 1
0.0788	m	0 0 2
0.1058	s	1 2 1
0.1085	s	0 3 0
0.1150	s	1 1 2
0.1289	w	0 2 2
0.1472	vw	2 2 0
0.1583	w	1 3 0

Table 5  
 $\text{Sc}_2\text{Ru}$  X-ray diffraction data

$\sin^2\theta$	Relative intensity	<i>h k l</i> planes
0.0316	s	0 2 2
0.0404	m	1 1 3
0.0644	w	0 0 4
0.0735	vw	1 3 3
0.0965	vw	4 2 2
0.1059	m	3 3 3
0.1241	w	0 4 4
0.1376	w	1 3 5
0.1440	m	2 4 4
0.1547	w	0 2 6
0.1696	w	3 3 5

1070 °C. The congruent nature of the crystallization of  $\text{Sc}_{57}\text{Ru}_{13}$  was derived from the shape of its liquidus curve (occurrence of the maximum at 1270 °C). This curve is plotted from the DTA data of the alloys with 10–23 at.% Ru (Table 2). In turn, this curve indicates the possible existence of a eutectic of the type  $\text{L} \rightleftharpoons \langle \beta\text{-Sc} \rangle + \text{Sc}_{57}\text{Ru}_{13}$ . However, metallography does not reveal a eutectic mixture in the cast alloys within this range of compositions (Fig. 2(c)). It may be a consequence of eutectic degeneration. The eutectic composition has nearly 12 at.% Ru. It was determined as the point of intersection of the  $\langle \beta\text{-Sc} \rangle$  and  $\text{Sc}_{57}\text{Ru}_{13}$  liquidus curves with the invariant horizontal line, corresponding to reaction  $\text{L} \rightleftharpoons \langle \beta\text{-Sc} \rangle + \text{Sc}_{57}\text{Ru}_{13}$ . The value of the reaction temperature is 1200 °C which was established on the basis of DTA data (Table 2). We observed characteristic effects in the heating and cooling curves of the 1–18 at.% Ru alloys, annealed at 900 °C, within the range of temperatures 1040–1060 °C. These effects and also the solid-phase transformation observed by metallographic analysis indicated the reaction to be eutectoid:  $\langle \beta\text{-Sc} \rangle \rightleftharpoons \langle \alpha\text{-Sc} \rangle + \text{Sc}_{57}\text{Ru}_{13}$ . The eutectoid composition can be expected to have between 2 and 5 at.% Ru, because the solubility of ruthenium in  $\beta$ -scandium reaches 5 at.%. This result follows from the position of the alloy with 5 at.% Ru at the end of the eutectic horizontal line, which displays very little effect in the heating and cooling curves at 1200 °C. The solubility of ruthenium in  $\alpha$ -scandium is assumed to be less than 1 at.%. This follows from the effects in the thermograms of this alloy at 1040 °C, corresponding to the transformations  $\langle \beta\text{-Sc} \rangle \rightleftharpoons \langle \alpha\text{-Sc} \rangle + \text{Sc}_{57}\text{Ru}_{13}$ .

As reported in [7], the X-ray diffraction investigation of cast samples of  $\text{Sc}_{44}\text{Ru}_7$  and samples annealed at 1023 K for 3 weeks of the same composition did not reveal the occurrence of a phase with  $\text{Mg}_{44}\text{Rh}_7$ -type structure, related to  $\text{Sc}_{44}\text{Os}_7$  and  $\text{Sc}_{44}\text{Ir}_7$ .

We examined a number of alloys within the range 10–17 at.% Ru after annealing for 200 h at 900 °C.

Besides the effects mentioned above, the DTA of these alloys revealed complementary effects at about 950 °C. Microprobe analysis of the alloy with 13.8 at.% Ru made it possible to detect the occurrence of a phase with Sc<sub>44</sub>Ru<sub>7</sub> stoichiometry in it and the occurrence of small amounts of Sc<sub>57</sub>Ru<sub>13</sub> (Table 3). The X-ray diffraction of this alloy is hampered because of the large size of the unit cells which leads to a large number of reflections of similar angular positions. Nevertheless, in the reflection angle range  $9^\circ < \theta < 20^\circ$  of the X-ray diagram of the considered sample one can single out independent reflections, belonging only to Sc<sub>57</sub>Ru<sub>13</sub> or only to Sc<sub>44</sub>Ru<sub>7</sub>. On the basis of the foregoing, one may suppose that Sc<sub>44</sub>Ru<sub>7</sub> forms in the Sc–Ru system by means of a solid state reaction at 950 °C (Fig. 1).

## References

- [1] V.B. Compton, *Acta Crystallogr.*, 12 (1959) 651.
- [2] A.E. Dwight, *Trans. Am. Soc. Met.*, 53 (1961) 479.
- [3] A.T. Aldred, *Trans. Metall. Soc. AIME*, 224 (5) (1962) 1082.
- [4] Ye. M. Savitskii and V.B. Gribulya, *Dokl. Akad. Nauk SSSR*, 190 (5) (1970) 1147.
- [5] Ye. M. Savitskii, V.P. Polyakova and N.B. Goryna, *Izv. Akad. Nauk SSSR, Met.*, 6 (1971) 161.
- [6] B. Chabot, K. Cenzual and E. Parthé, *Acta Crystallogr., Sect. B*, 36 (1980) 7.
- [7] B. Chabot, K. Cenzual and E. Parthé, *Acta Crystallogr., Sect. B*, 36 (1980) 2202.
- [8] K. Cenzual, B. Chabot and E. Parthé, *Acta Crystallogr., Sect. C*, 41 (1985) 313.
- [9] M. Pirani and H. Alterthum, *Z. Electrochem.*, 29 (1923) 5.
- [10] M. Cohen, *Rev. Sci. Instrum.*, 6 (1935) 68.
- [11] J. Hess, *Acta Crystallogr.*, 4 (1951) 209.